Limitations of the applicability of the concept of hybrid renewable energy source plant in practical implementation

DOI:
10.1049/icp.2021.1969

LIMITATIONS OF THE APPLICABILITY OF THE CONCEPT OF HYBRID RENEWABLE ENERGY SOURCE PLANT IN PRACTICAL IMPLEMENTATION

Ana Radovanović*, Jovica V. Milanović

Department of Electrical and Electronic Engineering, The University of Manchester, Manchester, UK
**ana.radovanovic@manchester.ac.uk*

Keywords: DYNAMIC MODELLING, ECONOMIC DISPATCHING, HYBRID RENEWABLE ENERGY SOURCE PLANT, TRANSIENT STABILITY

Abstract

Hybrid renewable energy source (HRES) plants have been recognized as a promising option for obtaining stable power production from renewable energy sources. The research on HRES plants has been mostly focused on the economic benefits of this concept. Much less attention has been paid to the influence of economic dispatch of HRES plants on system dynamic performance. This paper illustrates the necessity of defining the optimal technology mix in the HRES plant for certain system conditions from the perspective of both economy and system dynamic behaviour. In this study, the focus is on transient system stability. Furthermore, the methodology for developing dynamic equivalent of the whole HRES plant for transient stability studies in the form of a low-order transfer function model is presented. Illustrative results are obtained using an HRES plant consisting of several non-dispatchable renewable generation technologies.

1 Introduction

Unlike conventional power plants, renewable energy source (RES) plants are characterized by intermittent power output due to weather dependence. Hybrid renewable energy source (HRES) plants, comprising various renewable generation and storage technologies, have been seen as a promising solution to this issue. Namely, the HRES plant concept utilises the complementary properties of different technologies to compensate their deficiencies to a certain extent, and thus increases reliability of meeting operator requirements in terms of plant power production [1].

So far, the focus of the research on HRES plants has been on the optimal design and dispatch of HRES plants' individual components with the objective of minimizing total plant costs while satisfying the specified power production profile [1]. Much less attention has been paid to the influence of optimally dispatched HRES plant on power system dynamic performance and stability. In future power systems with a considerable number of integrated RES plants and decommissioned conventional power plants, optimal economic dispatch of HRES plants may violate system dynamic limits. In other words, system dynamic stability may become a determining constraint when deciding on HRES plant's technology mix (i.e., HRES plant composition) for a particular time period. Under such conditions, it might be necessary to make a shift from the traditional economic carbon reduction-driven dispatch of generation units only to the dispatch additionally governed by system dynamics/stability analysis.

Analysing the impact of HRES plants on the system stability requires their adequate dynamic representation. Full-scale dynamic modelling of each unit in HRES plants is impractical as it results in high-order mathematical model and requires, often unavailable, detailed data. As a result, dynamic equivalent models (DEMs) of large RES plants, i.e., the simplified versions of the full-scale dynamic models, have been recommended for modelling these plants in system stability studies [2].

This paper investigates the need for taking into account the dynamic characteristics of the HRES plant when deciding on the optimal HRES plant composition for a particular time period. The focus of the study is on transient system stability. In addition, the procedure for developing low-order transfer function (TF)-based DEM of HRES plant for transient stability analysis is presented. Unlike the reported equivalent modelling methodologies aimed at highly accurate modelling of dynamic responses of the plant [2], [3], the objective of this research was on developing DEMs that will not compromise the accuracy of the global transient system stability assessment. The focus was on the accuracy of the overall transient stability results as HRES plant power responses having different shape in time may result in similar transient stability behaviour. The test system involves an HRES plant containing three RES technologies.

2. Methodology

2.1 Analysing the Impact of HRES Plant Composition on Transient System Stability Status

The analysis on the influence of the technology mix in the HRES plant on the overall transient stability is based on a set of representative system loading conditions and HRES plant compositions. For the analysed loading level, the study identifies critical HRES plant penetration level (the minimum share of the HRES plant in covering the total system load) for taking into account the dynamic performance of the HRES plant, when defining the optimal plant composition. HRES plant penetration level is defined:

$$HRES_{Level}(\%) = 100 \times \frac{P_{HRES}}{P_{Load}}, \quad (1)$$

where P_{HRES} is the total HRES plant power output and P_{Load} is the total system load.

For the chosen loading level, the analysis starts with selecting initial value of $HRES_{Level}$, generating a set of random HRES plant compositions with the plant output calculated from (1), and assessing system stability for each plant composition in case of a number of self-clearing three-phase faults in the network. Three-phase faults are chosen as they usually result in the most severe conditions in the system. If the system is transiently unstable for a single fault simulation, the considered HRES penetration level is the critical HRES level for the analysed loading condition; otherwise $HRES_{Level}$ is increased and the above-described steps are repeated.

2.2 Methodology for Dynamic Equivalent Modelling of HRES Plants in Transient System Stability Studies

The flow chart of the methodology for equivalent modelling of HRES plants for transient stability studies is shown in Fig. 1 (inputs and outputs of the stages are marked by dashed rectangles). (*Note: The text describing features of equivalent modelling methodology is paraphrased from [4] as both papers rely on the same methodology*) The methodology is based on historical HRES plant production data, statistics about short-circuit faults in the network and unsupervised clustering methods. The proposed procedure is applicable to plants connected to distribution/transmission network level at a single point of common coupling (PCC). A DEM is developed for each group of HRES plant power responses resulting in similar transient system stability performance, regardless of dissimilarities in their shape.

In the first stage (block {2} in Fig. 1) the fuzzy c-means clustering method is applied to historical technology mixes in the HRES plant to identify characteristic plant compositions (block {3} in Fig. 1) during the year. Analysing only characteristic instead of all possible plant compositions provides computationally efficient procedure. Characteristic plant compositions correspond to cluster centroids defined by the fuzzy c-means algorithm. The optimal number of clusters in the historical data set, i.e., the number of typical plant compositions, is defined as the median of the numbers of clusters suggested by three widely applied clustering indicators - mean square error, clustering dispersion index, and mean index adequacy [5].

Case studies (CSs) reflecting the most probable annual HRES plant dynamic performance in transient stability studies are used for DEM development. The CSs are defined through a Monte Carlo (MC) procedure (block (5) in Fig. 1) based on typical plant compositions and network short-circuit fault statistics. In each MC simulation, uncertainties in the production and location of individual plants within the HRES plant are taken into account, while fault type, location and impedance are selected following the methodology presented in [6] and [7]. MC CSs are conducted in DIgSILENT/PowerFactory using the detailed HRES plant and network dynamic model (block {7} in Fig. 1). The simulated HRES plant power responses are analysed on the basis of their contribution to the transient system stability performance described by transient stability index (TSI) (block {9} in Fig. 1) [7]. Clusters of TSI values are defined using the Kernel Density Estimation (KDE) technique [8] (block {10} in Fig. 1), and CSs resulting in TSI values allocated to the same cluster are represented by a common DEM.

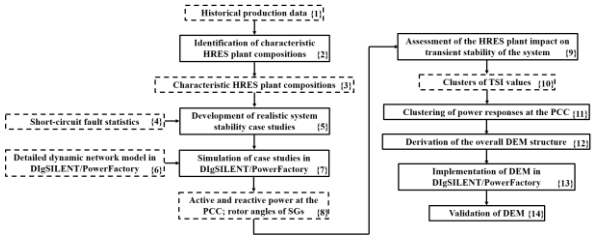

Fig. 1 The flow chart of the equivalent modelling methodology (adopted from [4])

Following this, HRES plant power responses are z-normalized as total HRES plant production varies across MC simulations and clusters of normalized responses (block {11} in Fig. 1) are formed knowing the allocation of MC CSs to TSI clusters. For each cluster, a representative CS is defined as the CS producing a representative response that corresponds to a cluster medoid (the response that is the most similar to the average of cluster responses). DEM structure is shown in Fig. 2. The real and reactive power responses of the HRES plant are produced by separate parts of the DEM but they have the identical structure given by (2):

$$z_{EQ,Y}(t) = \begin{cases} 0, & t < t_{fault} \\ z_{Fault,Y}, & t_{fault} \le t \le t_{clear}, \\ z_{TF,Y}(t), & t > t_{clear} \end{cases} \quad (2a)$$

$$Y_{EQ}(t) = Y_{SS} + z_{EQ,Y}(t) \times SD_Y^{rep}, \quad (2b)$$

where $z_{EQ,Y}(t)$ is the z-normalized power response of the model, t_{fault} is the moment of fault occurrence, t_{clear} is the moment of fault clearing, $z_{Fault,Y}$ is the value of z-normalized power response of the model during the fault, $z_{TF,Y}(t)$ is the z-normalized power response of the model after the fault clearance, $Y_{EQ}(t)$ is the power response at the

PCC in absolute units (after inverse z-transformation), Y_{SS} is the total power output of the plant before the disturbance, SD_{Yrep} is the standard deviation of the representative power response in absolute units. Simulation of z-normalized power responses using (2a) is represented by blue solid rectangles in Fig. 2. A TF is used for simulating plant response after fault clearing. Voltage and real and reactive power at the PCC are TF input and output signals, respectively. TF parameters are estimated through an iterative optimization procedure using voltage and z-normalized power response at the PCC obtained in the representative CS as TF input and output, respectively. Transformation of normalized into power responses in absolute units (blue dashed rectangles in Fig. 2) is performed according to (2b). Equation (2b) uses HRES plant production in steady state for a given plant composition and the standard deviation of the representative power response in absolute units in inverse normalization instead of the average and standard deviation of power response in absolute units, respectively, ([9]) as this information cannot be known in advance for an arbitrary operating condition and short-circuit fault.

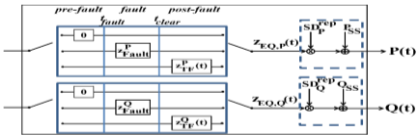

Fig. 2 The schematic diagram of DEM (adopted from [4])

Finally, DEM is connected to the network model in DIgSILENT/PowerFactory at the PCC (block {13} in Fig. 1). DEM accuracy is evaluated by comparing TSI values produced by the system with the detailed and equivalent plant model for a range of system conditions (block {14} in Fig. 1) as follows:

$$TSI_{Err}(\%) = 100 \times \frac{|TSI_{ORG} - TSI_{EQ}|}{TSI_{ORG}}, \quad (3)$$

where TSI_{ORG} and TSI_{EQ} are TSI values obtained using the detailed and equivalent HRES plant model, respectively.

3 Test System

The test system (modelled in DIgSILENT/PowerFactory [10]) is shown in Fig 3. (*Note: The following text is paraphrased from [4] as both papers use this test system*) The HRES plant contains a wind farm (WF), a photovoltaic (PV) plant and a run-of-river hydro power plant (HPP), and is connected to one of the load busses in the standard IEEE 9-bus model [11]. Models of individual plants in the HRES plant contain the dynamic model of a generation technology and its control system. All individual plants have the same capacity (210 MVA) to prevent any single technology dominating HRES plant dynamics. The HPP is represented by the standard fifth-order synchronous generator (SG) model, while IEEE DC1A exciter and IEEEG3 are used for modelling its governor and excitation system, respectively [12]. The PV plant and WF are represented by corresponding aggregate models obtained by scaling up the models of individual units [10]. In both plants, the number of individual units in service is defined by the total plant production as it is assumed that units in operation produce rated power output of 2 MW. Detailed description of PV plant and WF dynamic modelling is available in [7]. The total system load is represented by three loads in the transmission network (TN). Load A and B correspond to the 35% of the total load each and have a unity power factor, whereas the power factor of Load C is 0.95 (inductive).

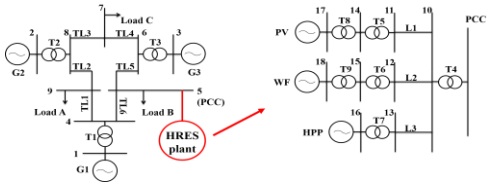

Fig. 3 The schematic diagram of the test system (adapted from [4])

4 Results and Discussion

4.1 Identifying Critical HRES Plant Penetration Levels

For this study, the values of inertia and reactances in d- and q-axis of the generator G1 in the TN (see Fig. 3) are set to new values: 3.55 s, 1.64 p.u., and 1.24 p.u., respectively, as the transient system stability status with the standard values given in [11] is insensitive to changes in HRES plant operating conditions. The analysis is carried out for five characteristic values of the total system load corresponding to the 10th, 25th, 50th, 75th and 90th percentile of the average annual loading profile of Central-Northern Italy for the period 2015-2018 [13] (the considered operating points are given in Table 1). Prior to the analysis, the data were scaled so that the maximum load level corresponds to the sum of rated active powers of SGs in the TN and the maximum HRES plant production. For the considered (fixed) loading level, HRES plant penetration level is gradually increased and a set of 200 random HRES plant compositions (a half of the compositions contains converter-connected technologies only, i.e., the PV plant and WF, as they are more prone to system instability) is generated for each analysed penetration level. In case of high value of $HRES_{Level}$, the number of random plant compositions can be lower than 200 due to small number of compositions capable of producing the required HRES plant production. Three-phase faults are simulated at the end and middle of TN lines. The power outputs of SGs in the TN are obtained from the optimal power flow with the objective of minimizing total power production costs. In order to take into account reduction in the total system inertia due to HRES plant production, each SG is assumed to represent an equivalent generator of a plant having the maximum four identical units in service at the same time. The minimum operating capacity of the plant for producing the specified power output is calculated as follows [7]:

$$MVA_{SG_i,Min} = \frac{P_{SG_i}}{(1-SCap_{SG_i}) \times Npf_{SG_i}}, \quad (4)$$

where P_{SGi} is the dispatch of the *i*-th SG in MW, $SCap_{SGi}$ is the spare reserve of the *i*-th SG in p.u. and Npf_{SGi} is the rated power factor of the *i*-th SG. A fixed spare capacity of 15% and a rated power factor of 0.85 are adopted [7]. The capacity calculated by (4) determines the maximum number of units in the plant that can be disconnected.

Table 1 also provides critical HRES plant penetration levels for the analysed loading conditions. Transient system instability that can occur for some HRES plant compositions at these penetration levels is characterized by undamped electromechanical oscillations. Dynamic characteristics of plant composition become relevant for transient system stability for high values of $HRES_{Level}$ - (64-69)%. In the case of high participation of the HRES plant in the total system production, large number of units in the conventional power plants can be disconnected, which in turn results in small system inertia level. The unstable cases occur when the technology mix in the HRES plant consists of converter-connected generators only. In the case of low loading conditions 1 and 2, the system is unstable for some fault locations (mostly the ones close to G3 in Fig. 3) when the share of the PV plant in the HRES plant output is between 25% and 60%, due to the interaction between the controllers of the PV plant and WF. In the case of the remaining loading levels, the system is unstable for all compositions without the HPP. Thus, for any loading level in the system, there is an $HRES_{Level}$ threshold above which different compositions with the same power output can result in different transient stability status, while the actual number of unstable cases depends on the presence of the HPP in the HRES plant, rotational reserve available in the rest of the system, and parameters of controllers of individual plants in the HRES plant.

Table 1 Analysed loading conditions, critical HRES plant penetration levels and the number of unstable cases

Loading condition	1	2	3	4	5
Total system load (MW)	330	373	457	564	623
Critical HRES plant penetration level (%)	66	64	67	69	65
Number of unstable cases (%)	4.2	6	50*	50*	50*

*HRES plant compositions without the HPP

4.2 Development of DEMs of the HRES Plant

The production data used in this analysis correspond to the total production of run-of-river HPPs, PV plants and WFs in Central-Northern Italy for the period 2015-2018 [13]. Prior to the analysis, the data were scaled down so that the maximum power output of each individual technology in the HRES plant during the analysed period corresponds to its rated power. The system load data correspond to the ones used in the previous study.

The application of the fuzzy c-means algorithm to the historical production data results in nine clusters of HRES plant compositions. Characteristic HRES plant compositions correspond to cluster centroids and are given in Table 2. Also, nine clusters of total TN load (and consequently nine typical loading levels) are defined according to time instance of historical load and production data samples. The MC procedure involves 1,000 MC simulations per typical HRES plant composition. In each set of 1,000 simulations, the production of each individual plant is uniformly varied in the range of ±5% around the typical HRES plant composition, while the lengths of lines connecting individual plants to the PCC are sampled uniformly between 0.5 km and 5 km. TN short-circuit fault data are adopted from [14] and [15]. Uniform probability distribution function is also used for selecting fault location along a line and sampling fault impedance from the range (0-20)Ω [16]. The plant responses are simulated for 10 s with the sampling rate of 1 ms and with a fault occurring at 1 s (fault duration was 100 ms in all MC CSs).

Table 2 Characteristic annual HRES plant compositions

Composition	PV (MW)	WF (MW)	HPP (MW)
1	7	27	141
2	4	17	45
3	6	19	90
4	63	22	71
5	91	17	40
6	5	84	34
7	9	94	138
8	2	16	0
9	8	93	81

TSI values, calculated for each MC simulation, can be grouped into two clusters according to the KDE approach, meaning two DEMs are required for representing the whole HRES plant in transient stability studies during the year. TSI clusters are shown in Fig. 4 (a) in the form of boxplots (outliers are marked by red asterisks, whereas whiskers cover 99.3% of data in the case of normal distribution). Almost all MC CSs generated on the basis of the typical annual HRES plant compositions 6, 7 and 9 (characterized by the WF loading of about 50%) belong to TSI cluster 2, i.e., they can be represented by DEM 2, while the remaining characteristic plant compositions can be modelled by DEM 1. Thus, the choice of DEM at any time during the year depends on plant composition only. The expected time of use of the DEMs during the year can be defined based on time instance of historical production data samples. DEM 1 could be used for modelling the HRES plant in transient stability studies during the whole year, except during the period January-March when both DEMs are adequate models for approximately the same number of days per month. Both DEMs contain 11 states, which represents a considerable model simplification as the detailed HRES plant model contains 44 differential equations. DEM accuracy is tested on both the trained data

(i.e., the data used for DEM development) and the test data for the analysed region for the year of 2020. Results of model evaluation are shown in Fig. 4 (b) in the form of cumulative distribution functions (cdfs). For the trained data set, the median TSI_{Err} indicator is 0.14%, while 90% of the CSs is characterized by TSI error lower than 0.4%. When it comes to the test data, model accuracy is slightly lower than in the case of trained CSs. Still, the 50th and 90th percentile of the cdf of TSI_{Err} indicator are 0.34% and 1.7%, respectively, which demonstrates high accuracy of the developed DEMs.

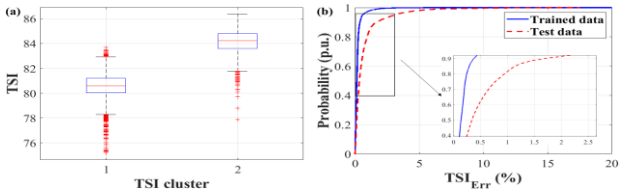

Fig. 4 (a) TSI clusters (adopted from [4]), (b) cdf of the error in TSI value for the trained (blue solid line) and test (red dashed line) data

5 Conclusion

The paper has illustrated the need for taking into account the dynamic behaviour of the HRES plant when deciding on the optimal technology mix in the plant for certain system conditions. When the HRES plant production exceeds its threshold, HRES plant composition cannot be defined on the basis of economy only. Reduction in the total system inertia (coupled with the consequential change in network electric parameters) and parameters of HRES plant controllers are the main factors determining the value of the critical HRES plant power output. Furthermore, the paper has presented the methodology for developing DEMs of HRES plants suitable for transient system stability assessment using TSI value. The proposed DEM is in the form of TF with voltage and real and reactive power at the PCC as input and output signals, respectively. DEMs developed for the test plant are characterized by high accuracy (the median TSI error is lower than 2%). Given that the order of DEMs is significantly lower than the full-scale plant model order, they can provide quick transient system stability assessment. In addition, the choice of the adequate DEM at any time during the year depends on the plant composition only, which also makes the presented procedure suitable for practical applications.

6 Acknowledgements

The research is supported by the EU H2020 project CROSSBOW (grant agreement 773430).

7 References

[1] Hina Fathima, A., Palanisamy K.: 'Optimization in microgrids with hybrid energy systems - a review', Renew. Sustain. Energy Rev., 2015, 45, pp. 431-446

[2] Zali, S.M., Milanović, J.V.: 'Generic model of active distribution network for large power system stability studies', IEEE Trans. Power Syst., 2013, 28, (3), pp. 3126-3133

[3] Chaspierre, G., Denis, G., Panciatici, P. et al.: 'An active distribution network equivalent derived from large-disturbance simulations with uncertainty', IEEE Trans. Smart Grid, 2020, 11, (6), pp. 4749-4759

[4] Radovanović, A., Milanović, J.V.: 'Equivalent modelling of hybrid RES plant for power system transient stability studies', IEEE Trans. Power Syst., early access, 13 August 2021, doi: 10.1109/TPWRS.2021.3104625

[5] Tsekouras, G.J., Kotoulas, P.B., Tsirekis, C.D. et al.: 'A pattern recognition methodology for evaluation of load profiles and typical days of large electricity customers', Electr. Pow. Syst. Res., 2008, 78, (9), pp. 1494-1510

[6] Li, W.: 'Risk Assessment of Power Systems: Models, Methods, and Applications' (John Wiley & Sons, Inc., 2nd edn. 2014)

[7] Papadopoulos, P.N., Milanović, J.V.: 'Probabilistic framework for transient stability assessment of power systems with high penetration of renewable generation', IEEE Trans. Power Syst., 2017, 32, (4), pp. 3078-3088

[8] Han, J., Kamber, M., Pei, J.: 'Data Mining Concepts and Techniques' (Elsevier Inc., 3rd edn. 2012)

[9] Mohamad, I.B., Usman, D.: 'Standardization and its effects on k-means clustering algorithm', Res. J. Appl. Sci. Eng. Technol., 2013, 6, (17), pp. 3299-3303

[10] 'DIgSILENT PowerFactory 2019 User Manual' (DIgSILENT GmbH, 2019)

[11] Zimmerman, R.D., Murillo-Sanchez, C.E., Thomas, R.J.: 'MATPOWER: Steady-state operations, planning, and analysis tools for power systems research and education', IEEE Trans. Power Syst., 2011, 26, (1), pp. 12-19

[12] Kundur, P.: 'Power system stability and control' (McGraw-Hill, 1994)

[13] 'ENTSO-E Transparency Platform', https://transparency.entsoe.eu, assessed 15 January 2021

[14] Zhang, Y.: 'Techno-economic Assessment of Voltage Sag Performance and Mitigation'. PhD thesis, The University of Manchester, 2008

[15] Leborgne, R.C., Olguin, G., Carvalho Filho, J.M., et al.: 'Differences in voltage dip exposure depending upon phase-to-phase and phase-to-neutral monitoring connections', IEEE Trans. Power Del., 2007, 22, (2), pp. 1153-1159

[16] Cebrian, K.C., Camilo, L., Kagan, N., et al.: 'Consideration of voltage sags disruption risks in distribution planning studies'. Proc. CIRED 18th Int. Conf. Electr. Distrib., Turin, Italy, June 2005, pp. 1-4